POLYTWIN PRECIPITATES

IN DECOMPOSED HYPER-EUTECTOID CuBe ALLOYS

B. Cheong, K. Hono† and D. E. Laughlin

Dept. of Materials Science and Engineering
Carnegie Mellon University
Pittsburgh, PA 15213

† Institute for Materials Research
Tohoku University
Sendai 980, Japan

Abstract

We have examined the polytwin precipitates which are encountered during decomposition of a hyper-eutectoid CuBe alloy; (β(*bcc*) -->γ(B2) + α(*fcc*)). We show that the polytwin morphology characterized by a sawtooth shape derives from a remarkable interplay between thermodynamic and kinetic factors, that is, between the instability of the initial decomposition product (designated as α' (*fct*)) and the kinetic advantage effected by intersection of the α' plates. In terms of an atomistic mechanism, the morphology renders itself as a fine illustration of the interplay between diffusional and displacive atomic motion. From experiments on kinetic path dependence and by comparison with the theoretical polytwin morphology, it is suggested that the sawtooth morphology is metastable and does not satisfy the invariant plane strain condition.

Twinning in Advanced Materials
Edited by M.H. Yoo and M. Wuttig
The Minerals, Metals & Materials Society, 1994

Introduction

In a phase transformation involving a crystal lattice rearrangement, a new phase morphology often appears which consists of alternating domains of different crystallographic variants in twin orientations. It is well-known from previous studies that the appearance of such a polytwin complex is driven by the tendency to better accommodate the symmetry-breaking transformation strain accompanying a crystal lattice rearrangement. This rudimentary character of a polytwin complex may become manifested through different formation mechanisms and into different specific morphological forms, depending on the thermodynamic and kinetic nature of a phase transformation.

Herein, we report on the polytwin morphology which is encountered during precipitation in a hyper-eutectoid CuBe alloy. Decomposition of a β(*bcc*) phase hyper-eutectoid CuBe alloy into a two phase (γ(B2)+α(*fcc*)) mixture (1) represents an interesting class in which a drastic change in the crystal lattice (*bcc* to *fcc*) is accompanied by diffusional atomic reconfiguration processes such as composition separation and *bcc* to B2 atomic ordering. This complex nature of the decomposition reaction leads to a thermodynamically and kinetically unconventional transformation path which, in turn, gives rise to an interesting precipitate morphology characterized by a polytwin plate of a sawtooth shape. Recently, we have conducted an experimental investigation of this (2,3). We summarize here some of the salient results.

Experimental procedure

The as-cast Cu-9.04 wt.%Be (41.2 at.% Be) binary alloys furnished by BrushWellman Inc. were homogenized for one day at 840 °C. The alloys were then sliced into pieces about 0.5 mm thick and were subsequently cold-rolled to about 0.2 mm thick. After further reduction in thickness down to about 0.1 to 0.15 mm by mechanical polishing, discs of 3 mm in dia. were punched out and were given a disordering treatment at 840 °C for 1 hour. The disordered specimens were either rapidly quenched into iced-brine water or air-cooled to room temperature outside the furnace. Quenched specimens were aged in a three zone Lindberg furnace. For all the heat treatments, samples were encapsulated in either quartz or pyrex tubes which were back-filled with argon. Specimens for TEM study were prepared using a twin-jet electro-polisher with an electrolyte of 70 vol. % methanol and 30 vol. % nitric acid below -30 °C and at 10 V. Conventional TEM was performed using a Philips 420T microscope operating at 120 kV. High Resolution TEM was conducted with JEOL 4000EX microscope at 400 kV.

Results and Discussions

Early Stage Transformation Microstructures and Polytwin Precipitate Morphology

The kinetics of precipitation in a hyper-eutectoid CuBe alloy is markedly fast and a conventional water-quenching has always led to the formation of very fine scale two phase microstructures. This is shown in Fig.1. Inspection of the TEM photographs reveals that the microstructures consist of the B2 ordered (γ) matrix and coherent platelike precipitates with habit planes close to $\{001\}_\gamma$. From the basic pattern of the SADP (Fig. 1c)), one can notice that the precipitate phase, constrained by $\{001\}_\gamma$ habit planes, is in Bain lattice correspondence with the matrix phase; hence it has the constrained crystal structure of *fct* (α').† The observed microstructures, in fact, resemble the ones resulting from an isostructural decomposition in a cubic alloy except for fault-like features inside the precipitate plates. These fault-like features can be seen in places where two orthogonal precipitate plates intersect with each other. On close examination, these faults are found to be, by large, stacking faults but some of them turn out to be very thin twin domains. This is shown in Fig. 2 by enlarged atomic resolution images of the planar faults marked A and B in Fig. 1a). From these images, a suggestion may be made regarding the formation mechanism of the twin domains, namely that the twin domains nucleate through the formation of stacking faults due to plate intersection. The DF image shown in Fig. 3. was taken from another water-quenched alloy (the quenching rate turned out to be slower than in the case of Fig. 1). In this micrograph, thin twin domains are imaged as thin bright areas in one set of plates and thin dark areas in the other set. From this change in predominant planar faults from stacking faults to twin domains with quenching rate, it appears that growth of twin domains is a diffusion-controlled

† A careful analysis of the SADP and TEM micrographs shows that habit planes are slightly rotated from $\{001\}_\gamma$ planes and the crystal structure is thus slightly deviated from *fct* by a monoclinic distortion: see the reference (3) for detailed discussion.

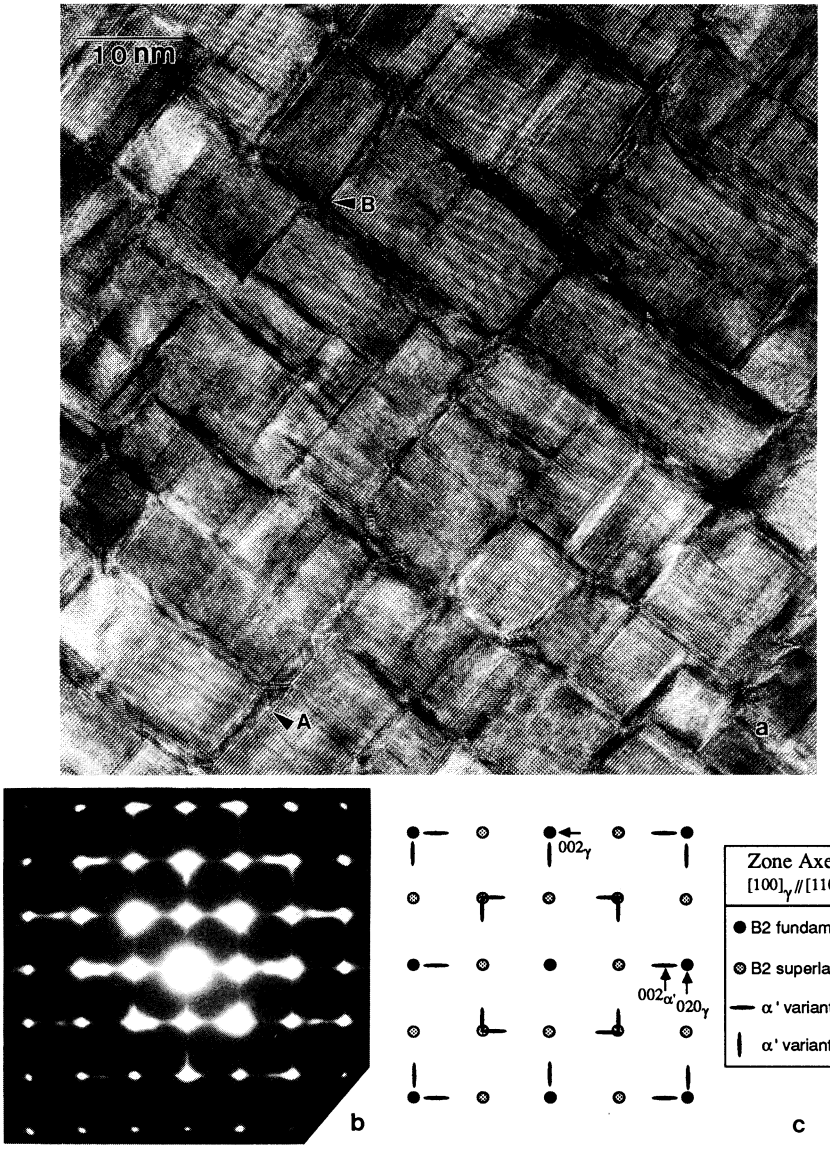

Figure 1: TEM photographs taken from the as-quenched state. (a) Many beam lattice image taken along $[100]_\gamma$ // $[110]_{prec.}$ (b) $[100]_\gamma$ zone axis SADP. (c) Schematic illustration of the basic pattern of the SADP. Notice a two phase state consisting of B2 ordered (γ) matrix and coherent platelike precipitates with habit planes close to $\{001\}_\gamma$.

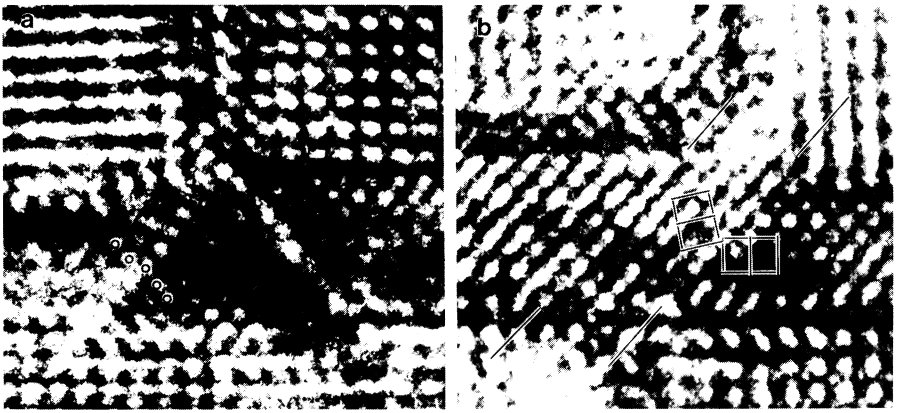

Figure 2: Atomic resolution images of the regions of plate intersection marked A and B in Figure 1a). (a) A: stacking fault. (b) B; twin domain.

Figure 3: Microstructure of the water-quenched alloy, quenched accidentally slower than the case of Figure 1. Notice thin bright and dark regions in two different sets of plates which depict twin domains in a respective set.

process, though nucleated by a shearing process. More detailed discussion of the twin formation mechanism is presented elsewhere (3).

Thermodynamic Origin of the Observed Polytwin Morphology

The microstructural features described above can be properly understood in terms of the phase diagram characteristics of the CuBe system with elasticity effects taken into account. A portion of the CuBe phase diagram (4) is schematically shown in Fig. 4a) with characteristic lines added and/or extrapolated. The lines denoted by T_c and T_{cs} represent the critical temperature line of A2 --> B2 ordering transition and conditional spinodal line (5), respectively. T_o is the temperature where the free energy of the α (*fcc*) phase is the same as that of the β(*bcc*) phase. A chemical free energy vs. composition diagram is shown in Fig. 4b) that represents the phase diagram characteristics at an arbitrary low temperature T_A below the eutectoid temperature. According to these diagrams, the equilibrium precipitate α phase would result from an undercooled β phase of the composition c^β along the following path;

(1) *A* ---> *B*: *bcc* to B2 atomic ordering.
(2) *B*---> *C*: isostructural decomposition leading to the formation of Cu-rich G.P. zones.
(3) *C*---> *D*: *bcc* to *fcc* crystal lattice rearrangement to form α' (*fct*) precipitates.
(4) *D*---> *E*: relaxation of the α' precipitates to the equilibrium α (*fcc*) precipitates.

With regard to the morphology of the precipitate plates, two points should be emphasized. Firstly, the Cu-rich G. P. zones resulting from the step 2 are of the plate shape and of the $\{001\}_\gamma$ habit planes. These are the direct consequences of the minimization of the elastic strain energy, given that the elastic anisotropy of the B2 phase is negative (6). This is illustrated in Fig. 5a). Constrained by $\{001\}_\gamma$ habit planes, the crystal lattice of the G. P. zones is distorted tetragonally along the $<001>_\gamma$ directions and this, in effect, accommodates a part of the Bain strain even prior to the onset of step 3. Secondly, the α' precipitates with the $\{001\}_\gamma$ habit planes due to step 3 are elastically unstable. This is illustrated in Fig. 5b). As compared with the minimum in Fig. 5a), one can see a local maximum along the $[001]_\gamma$ direction which signifies instability. This unstable nature of the α' precipitate leads to a rapid development of the processes which prompt a further relaxation of the Bain strain. These processes include habit plane rotation and the formation of polytwin domains.

Kinetic Transformation Path Dependence

In order to examine further the nature of the observed polytwin morphology, an experiment was carried out by employing two different heat treatments which influence kinetic path of the transformation and thus possibly, precipitate morphology: air-cooling and quench/aging. The results are shown in Fig. 6. The TEM BF micrograph shown in Fig. 6a) was taken from an air-cooled alloy. A network of polytwin precipitate plates which have a characteristic sawtooth morphology can be observed. These precipitate plates are identical in nature with, but more developed than the ones depicted in Fig. 3. To summarize the salient features; plates are aligned overall along the [010] and the [001] directions of the matrix γ phase but consist of interspersing, broad and thin individual segments of twin orientation which are rotated from the $[010]_\gamma$ or the $[001]_\gamma$ orientation. The habit planes are found to be approximately $(0\bar{1}3)_\gamma$ for the segments indicated by arrows. The precipitate morphology in aged alloys was examined by use of alloys aged at 300 °C for 24 hrs followed by water-quenching. In contrast to the well-developed sawtooth morphology of the air-cooled alloys, one can notice from Fig. 6b an array of individual precipitate plates, each having its respective habit plane rotated globally over the whole plate. From tilting experiments, the habit planes are found to be once again of the $(0hk)_\gamma$ type, specifically $(0\bar{1}3)_\gamma$ on average.

The difference in precipitate morphologies which was effected by a change in heat treatment scheme can be understood also with aid of the phase diagram of Fig. 4. In the case of air-cooling, a decomposing alloy stays longer in the (*bcc*+B2) two phase field and this prolonged isostructural decomposition would lead to a significant coarsening of the Cu-rich $\{001\}_\gamma$ G. P. zone plates before step 3 (C -->D) sets in. A global habit rotation of a large α' precipitate plate is then clearly kinetically unfavorable since it would require an extensive solute redistribution. In the presence of an effective twin nucleation mechanism (*i.e.* plate intersection), a large α' plate would instead form a polytwin plate and rotate the habit planes segment-wise. The situation is different in the quenched/aged alloys. Very fine precipitate plates, inherited from as-quenched states, are yet to grow as well as to relax the Bain transformation strain during the aging process. It is reasonable to expect that fulfilling both these

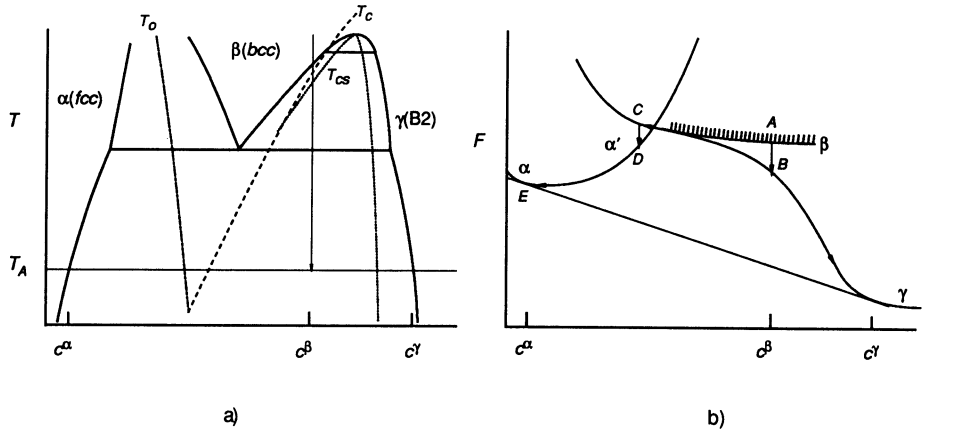

Figure 4: (a) Schematic of the CuBe phase diagram (see text for various characteristic temperatures). (b) Chemical free energy vs. composition diagram consistent with the phase diagram features at an arbitrary low temperaure T_A below the eutectoid point. When undercooled to T_A, a disordered β (*bcc*) phase of composition c^β would decompose along the path *A* --> *B* --> *C*--> *D* --> *E* to produce α (*fcc*) precipitates.

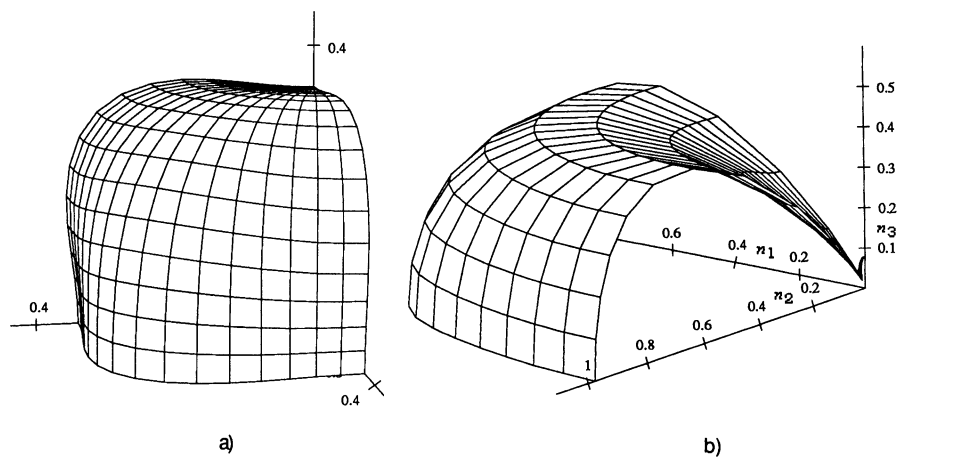

Figure 5: Octants of the elastic strain energy surface as a function of habit plane normal of a platelike precipitate embedded in the B2 matrix (strain energy is in an arbitrarily normailzed unit). (a) G. P. zone case and (b) *fcc* case. Notice that elastic energy along the $[001]_\gamma$ direction changes from a minimum (a) to a local maximum (b).

needs while preserving the sawtooth morphology is mechanistically hardly possible and thus a global rotation of the habit plane would be favored in this case.

Comparison with Theoretical Polytwin Morphology

It is noted that the sawtooth morphology of the polytwin plates, as we observed in continuously cooled CuBe alloys, is distinct from the conventional one which has been much discussed in regard to a stress free polytwin morphology that satisfies the invariant plane strain condition. The conventional morphology predicted by the elasticity theory of polytwin morphology (7,8) or equivalently from the theories of twinned martensite (9), is schematically shown in Fig. 7. Calculation was made for a polytwin plate which is made up of the same two variants that constitute the sawtooth morphology shown in Fig. 6, that is, two variants which have the axes of Bain distortion parallel to [010] and [001] directions of the matrix phase. One can notice that the observed morphology differs in the overall habit direction but even the directions of the segments are not consistent with that of the theoretical morphology. From this and from the experimental results described in the preceding section, it follows that a polytwin plate of the sawtooth morphology may be no more than a kinetic variant of a single domain plate with globally rotated habit plane which may not be able to offer further reduction in elastic strain energy than what could be achieved by a single rotated plate.

Acknowledgements

We are thankful to Prof. Khachaturyan for his interest in our study and for helpful discussions and to Prof. J. M. Howe of Univ. of Virginia for his help on the High Resolution TEM study. We also gratefully acknowledge the BrushWellman Inc. for a fellowship and for providing the CuBe alloys.

References

1. T. Tadaki, T. Sahara and K. Shimizu, " Electron Metallography of the Decomposition Processes in a Hyper-eutectic Cu-Be β Phase Alloy", Trans. Japan Inst. Met., 14 (1973), 401-407.

2. B. Cheong, K. Hono and D. E. Laughlin, " Transformation Path Dependence of the Bain Strain Relaxation during Decomposition of a Hyper-eutectoid CuBe Alloy", Metall. Trans A., 24, (1993), 2605-2611.

3. B. Cheong, K. Hono and D. E. Laughlin, " Bain Strain Relaxation during Early Stage Decomposition of a Hyper-eutectoid CuBe Alloy", Acta metall. mater., in press; B. Cheong, "Cubic to Tetragonal Crystal Lattice Reconstruction during Ordering or Decomposition", (Ph.D. thesis, Carnegie Mellon Univ., Pittsburgh, 1992), Chap 5.

4. D. J. Chakrabarti, D. E. Laughlin and L. E. Tanner, "The Be-Cu System", Bull. Alloy Phase Diagrams, 8 (1987), 269-282.

5. S. M. Allen and J. W. Cahn, "Mechanisms of Phase Transformations Within the Miscibility Gap of Fe-Rich Fe-Al Alloys", Acta metall., 24 (1976), 425-437.

6. A. G. Khachaturyan and D. E. Laughlin, "Structural Trnasformations during Decomposition in CuBe Alloys", Acta metall. mater., 38 (1990), 1823-1835.

7. A. G. Khachaturyan and G. A. Shatalov, "Theory of Macroscopic Periodicity for a Phase Transition in the Solid State", Sov. Phys. JETP, 29 (1969), 557-561; A. G. Khachaturyan, Theory of Structural Transformations in Solids (New York, NY: John Wiley & Sons, 1983), Chap 11.

8. A. L. Roitburd, " The Domain Structure of Crystals Formed in the Solid Phase", Sov. Phys. Solid State, 10 (1969), 2870-2876; A. L. Roitburd, " Domain Structure Caused by Internal Stresses in Heterophase Solids", Phys. Stat. Sol., 16 (a) (1973), 329-338.

9. M. S. Wechsler, D. S. Lieberman, and T. A. Read, "On the Theory of the Formation of Martensite", Trans. Met. Soc. AIME, 197 (1953), 1503-1515.

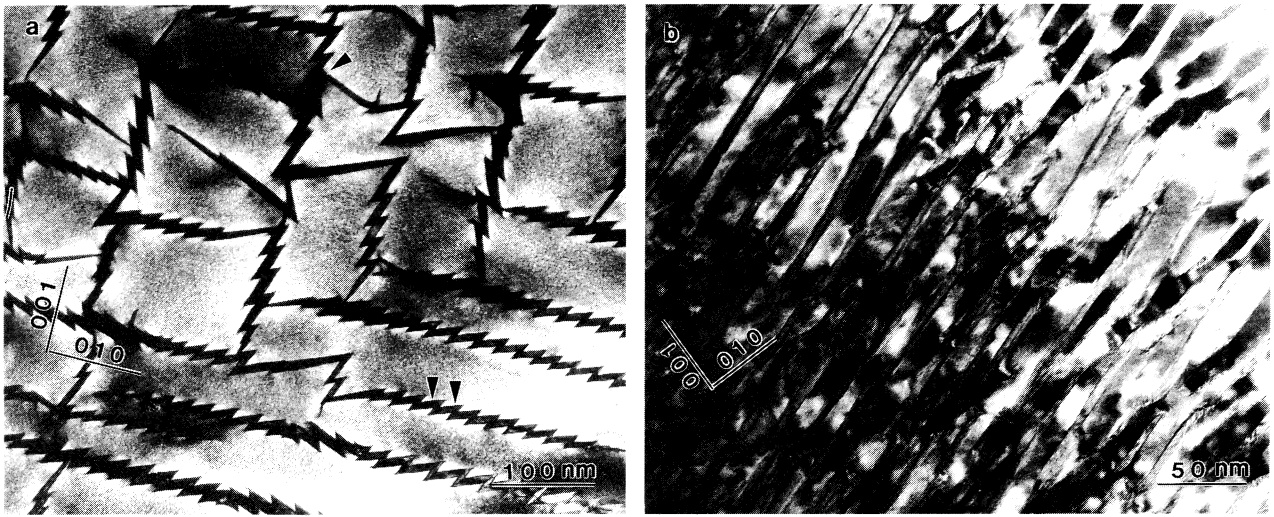

Figure 6: TEM Bright Field micrographs taken from (a) an air-cooled alloy and from (b) an alloy aged at 300 °C for 24 hours followed by water-quenching. Notice a remarkable difference in precipitate morphology between the two cases.

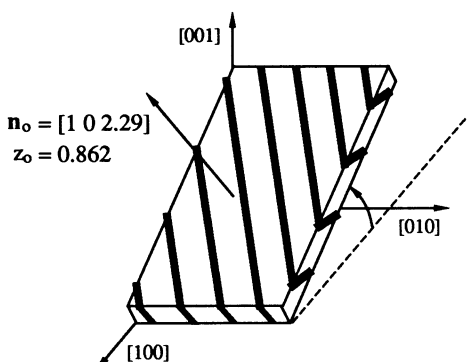

Figure 7: Theoretical morphology of a polytwin plate consisting of two precipitate variants, each having the axis of Bain distortion respectively parallel to the [010] and the [001] direction of the matrix phase.